Structural Engineering and Mechanics, Vol. 37, No. 1 (2011) 111-129
DOI: http://dx.doi.org/10.12989/sem.2011.37.1.111

Response of lap splice of reinforcing bars confined by FRP wrapping: application to nonlinear analysis of RC column

Amorn Pimanmas*[1] and Dam Xuan Thai[2]

[1]*Sirindhorn International Institute of Technology, Thammasat University, Pathum Thani 12121, Thailand*
[2]*Civil Engineering Department, The National University of Civil Engineering, Hanoi, Vietnam*

(Received September 28, 2009, Accepted September 13, 2010)

Abstract. This paper presents a nonlinear analysis of reinforced concrete column with lap splice confined by FRP wrapping in the critical hinging zone. The steel stress-slip model derived from the tri-uniform bond stress model presented in the companion paper is included in the nonlinear frame analysis to simulate the response of reinforced concrete columns subjected to cyclic displacement reversals. The nonlinear modeling is based on a fiber discretization of an RC column section. Each fiber is modeled as either nonlinear concrete or steel spring, whose load-deformation characteristics are calculated from the section of fiber and material properties. The steel spring that models the reinforcing bars consists of three sub-springs, i.e., steel bar sub-spring, lap splice spring, and anchorage bond-slip spring connected in series from top to bottom. By combining the steel stress versus slip of the lap splice, the stress-deformation of steel bar and the steel stress-slip of bars anchored into the footing, the nonlinear steel spring model is derived. The analytical responses are found to be close to experimental ones. The analysis without lap splice springs included may result in an erroneous overestimation in the strength and ductility of columns.

Keywords: tri-uniform bond stress model; nonlinear modeling; fiber-reinforced polymer; fiber discretization; lap splice spring.

1. Introduction

The seismic evaluation of existing reinforced concrete buildings requires an accurate treatment of various aspects of substandard reinforcement detailing in reinforced concrete components. According to the investigation of existing buildings constructed prior to 1970 around the world (Chai *et al.* 1991, Melek *et al*. 2003), the lap splices in substandard columns were typically short and were poorly confined by small amount of transverse steels. As a consequence, the stress in reinforcing bars cannot develop to yield level and the column may fail by brittle splitting failure which causes low strength and ductility. Some experimental researches have been conducted to examine the use of fiber reinforced polymer in the form of sheet wrapping around the critical lap splice zone to rehabilitate the column (Xiao and Ma 1997, Bousias *et al.* 2006, Harajli 2008). Because of the confinement effect, the bond strength is enhanced and the strength of lap splice can

*Corresponding author, Associate Professor, E-mail: amorn@siit.tu.ac.th

be developed into yielding range without premature splitting failure. There are however limited works dealing with the nonlinear analysis of RC columns taking into account the substandard lap splice (Cho and Pincheira 2006, Kim *et al*. 2006, Matrin 2007, Ogura *et al*. 2008) and confined ones (Binici and Mosalam 2007). One possible reason is that currently no bond stress model exists that can accurately predict the strength of lap splice. The nonlinear analysis of reinforced concrete buildings needs to properly include the effect of lap splice in order to assess the performance of both existing and retrofitted columns.

In the companion paper, the tri-uniform bond stress model has been developed to derive the equation for the strength of lap splice. It is noted that not only the strength of lap splice can be estimated but the entire steel stress-slip relation can also be constructed by combining the equilibrium, strain-slip relation and the constitutive bond stress slip model for each zone. The steel stress-slip relation is useful in the nonlinear static and dynamic analysis of RC column with unconfined and confined lap splices. By incorporating this model into the nonlinear frame analysis, it is possible to capture lap splice failure and an additional flexibility due to lap splice slip. This can enhance the accuracy of the frame analysis in the performance evaluation of existing and strengthened columns and the entire structures. The purpose of this paper is to present a general nonlinear modeling of RC column with particular attention on the confined lap splice modeling, to demonstrate the importance of incorporating the steel stress-slip relation in the analysis and to provide a verification of the tri-uniform bond stress model at a structural level where the experimental data are more readily available from cyclic tests of RC columns reported in literature. Even though the nonlinear analysis of cyclic response of RC column has included other effects besides bond matters, it is still of great value to strengthen the verification at the constitutive levels conducted in the companion paper. The hypothetical analyses that do not consider the effect of lap splice are also conducted to illustrate the importance of incorporating the steel stress-slip relation in the analysis.

2. Nonlinear modeling of RC column with lap splice confined with FRP

2.1 Modeling scheme

A nonlinear model of a reinforced concrete column is shown in Fig. 1 (Matrin 2007). This model represents a column under a single-curvature test set-up with the plastic hinge forming at the base. The model is divided into two parts denoted as elastic and plastic zones. The elastic zone is modeled by an elastic frame element of $H-L_p$ length to represent the elastic behavior of the column. The plastic zone is developed at the base of the column to represent the plastic yielding and other nonlinear effects concentrated at the column base. The plastic zone is modeled by a zero-length fiber section which is represented by a set of nonlinear springs to represent the concrete and reinforcement responses. The elastic and plastic parts are connected together by a rigid link of L_p length where L_p is the length of plastic hinge.

The elastic frame element is used to simulate flexural and axial stiffness in the elastic part. As recommended by ATC-40 (1996), the effective flexural rigidity is set to $0.7E_cI_g$; the effective axial rigidity is set to $1.0E_cA_g$; the effective shear stiffness is equal to $0.4E_cA_g/(H-L_P)$. The elastic modulus of concrete E_c is set to $4700\sqrt{f_c'}$ (MPa) as recommended by ACI318 (2005), in which, f_c' is the compressive strength of unconfined concrete (MPa); A_g and H are gross sectional area and

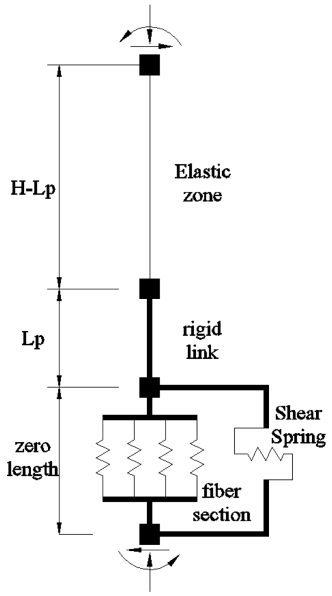

Fig. 1 RC column model

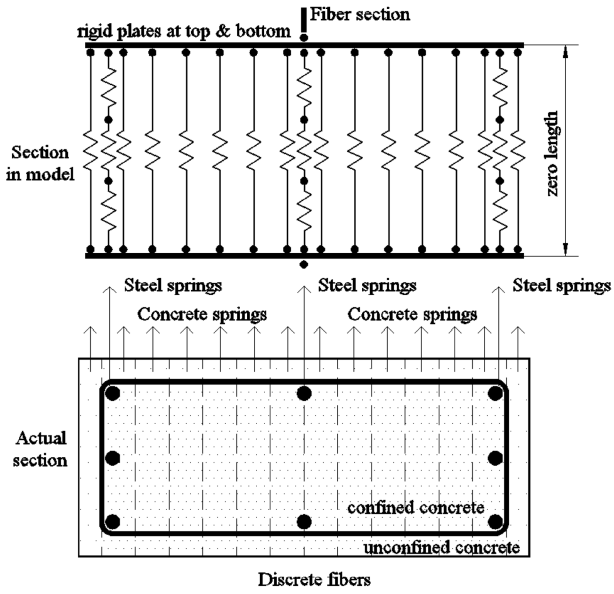

Fig. 2 Fiber section discretization

height of the column, respectively.

A fiber section is divided into a number of discrete fibers (Fig. 2). Each fiber is modeled as either concrete or steel spring or both, whose characteristics can be calculated from the section of fiber and material properties. In line with the zero-length fiber concept, the nonlinearity is assumed to be lumped or concentrated at the column base. The nonlinear behavior is manifested through a set of uniaxial springs that represent concrete and steel nonlinearity. In this modeling scheme, the constitutive laws of concrete and steel springs have to be expressed in terms of the relations between uniaxial stresses and displacements. The conventional uniaxial stress-strain constitutive laws can be converted (or lumped) to uniaxial stress-displacement relation by multiplying strain with plastic hinge length. Thus, in order to formulate the stress-displacement relation for spring, the plastic hinge length and relevant stress-strain constitutive laws of concrete and steel are required.

The concrete springs are classified into confined concrete and unconfined concrete. As can be seen from Fig. 2, the confined concrete is to model concrete core enclosed by the stirrups and the unconfined concrete is to model concrete cover. Thus, two parallel springs with different constitutive properties are used to represent confined concrete and concrete cover, respectively. The steel spring that represents the reinforcement in each fiber (Fig. 3) is assumed to consist of three sub-springs, namely, steel bar sub-spring, lap splice sub-spring, and anchorage bond-slip sub-spring connected in series from top to bottom. The steel bar sub-spring is to model the uniaxial stress-strain relation of steel bar. The lap splice sub-spring is to model the steel stress-slip relation of the lap splice. The anchorage bond-slip spring is to model the anchorage stress-slip relation of bars embedded into footing. The uniaxial stress-strain relation of steel bar is generally obtained from uniaxial tensile test of steel samples. It can be converted to uniaxial stress-displacement for steel bar sub-spring by multiplying strain with plastic hinge length as described. As for the lap splice spring and anchorage bond slip spring, the uniaxial stress-slip relations can be directly adopted as uniaxial stress-displacement relations of corresponding springs. The detailed formulations of uniaxial stress-

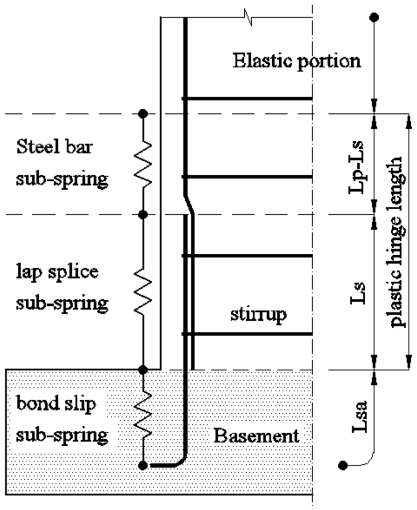

Fig. 3 Modeling of reinforcing bar by three sub-springs

slip relations are described in the companion paper.

Within the zero length fiber section, a shear spring is introduced to simulate the shear behavior in the column critical zone. In this study, the elastic shear stiffness is applied since the study focuses on the lap splice behavior. The backbone envelopes for uniaxial constitutive laws of these nonlinear springs taking into account the effect of FRP confinement are described in the next section. The nonlinear modeling scheme outlined here is implemented in a RUAUMOKO2D program (Carr 1998, 2005) for a general static and dynamic analysis of RC frame structures. Ruaumoko2D is a well known platform for analyzing reinforced concrete structures, especially with the capacity of degradation simulation and a huge database of hysteresis models embedded in the program.

The proposed modeling scheme can be conveniently implemented in Ruaumoko2D program. Ruaumoko2D provides zero-length nonlinear hysteretic spring elements where the uniaxial stress-displacement can be assigned for both envelope curve and hysteretic loops. The program also contains the standard elastic frame element and rigid link which can be used in elastic zone of the column and the connection between elastic and plastic zone (see Fig. 2), respectively.

2.2 Length of plastic hinge region

Priestley and Seible (1991) suggested the following plastic hinge length formulas for analyzing inelastic flexural behaviors of reinforced concrete columns with and without FRP jacketing

$$\text{Without FRP jacketing} \quad L_p = 0.08H + 0.022d_b f_y \tag{1}$$

$$\text{With FRP jacketing} \quad L_p = g + 0.044d_b f_y \tag{2}$$

Where g is a gap at the bottom of the jacket; d_b and f_y are diameter and yield strength of reinforcing bar, respectively.

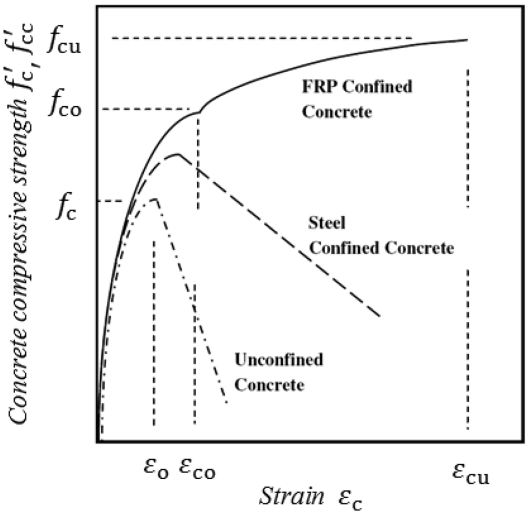

Fig. 4 Uniaxial stress-strain model of concrete (Harajli 2006a)

Xiao *et al.* (1997) slightly modified the above equations by replacing f_y with f_s based on an assumption that plastic hinge length was assumed to vary with stress f_s in the extreme tensile bar. The Eqs. (3) and (4) have the same format as Eqs. (1) and (2) but use variable steel stress f_s in place of the yield strength f_y

$$\text{Without FRP jacketing} \quad L_p = 0.08H + 0.022 d_b f_s \tag{3}$$

$$\text{With FRP jacketing} \quad L_p = g + 0.044 d_b f_s \tag{4}$$

2.3 Uniaxial constitutive laws of nonlinear springs

2.3.1 Concrete spring

The nonlinear force-deformation relation of concrete spring can be obtained from uniaxial stress-strain relation of concrete. Because FRP confinement provides additional lateral pressure, the compressive strength of concrete is increased (Fig. 4) (Harajli 2006a). The peak compressive force of a concrete spring F_c depends on the area of concrete in a fiber A_c and the confined compressive strength of concrete f_{cc}' which can be obtained from unconfined compressive strength f_c' multiplied by a confinement factor K as

$$F_c = f_{cc}' A_c \tag{5}$$

$$f_{cc}' = K f_c' \tag{6}$$

The calculation of the confinement factor K follows a uniaxial stress-strain model in Eqs. (7) and (8) for confined concrete with either FRP or transverse reinforcement as proposed by Harajli (2006a) and Harajli *et al.* (2006). The formula are applicable to both rectangular and circular cross section, partial and full wrapping, and types of steel stirrup (spiral or hoop) (Harajli 2006a, and Harajli *et al*. 2006). In Eqs. (7) and (8), A_{cc} is the area of concrete core; A_g is the area of gross

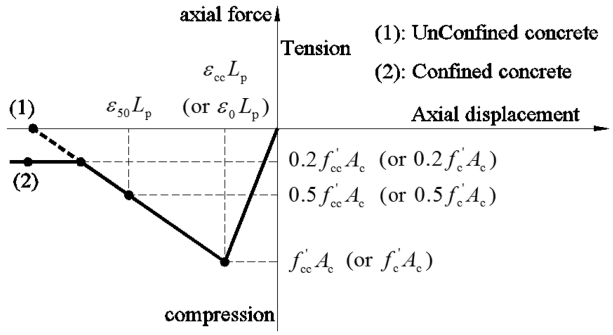

Fig. 5 Backbone curve for concrete spring

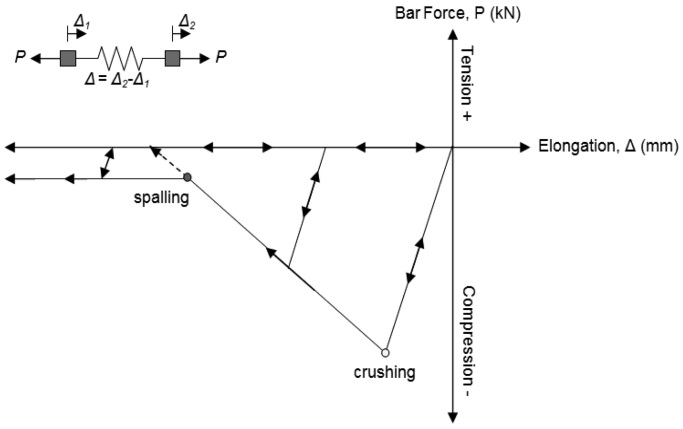

Fig. 6 Hysteretic model Bi-linear with Slackness (Carr 2005) for concrete springs

section; f_{lf}; f_{ls} are lateral passive confining pressure exerted by FRP and ordinary transverse steels respectively, k_1; k_2 are confinement effectiveness coefficients.

$$f'_{cc} = f'_c + k_1\left(f_{lf} + f_{ls}\frac{A_{cc}}{A_g}\right) \tag{7}$$

$$\varepsilon_{cc} = \varepsilon_o\left(1 + k_2\left(\frac{f'_{cc}}{f'_c} - 1\right)\right) \tag{8}$$

$$\varepsilon_{50} = \frac{3 + 0.002\,f'_c}{f'_c - 1000}\ (psi) \tag{9}$$

The degradation curve of a concrete spring is assumed to follow a linear line from the peak to a point of 50% remaining peak stress with the corresponding strain ε_{50} (Roy and Sozen 1965). The backbone curve that governs the behavior of concrete spring (confined or unconfined) is illustrated in Fig. 5. The cyclic behavior of the concrete springs is controlled by the hysteretic model "Bi-linear with Slackness" (Fig. 6) which is available in Ruaumoko 2D (Carr 2005). The stiffness of the unloading and reloading curve is assumed to be equal to that of the envelope. This model is thus a simplified one without consideration of stiffness degradation.

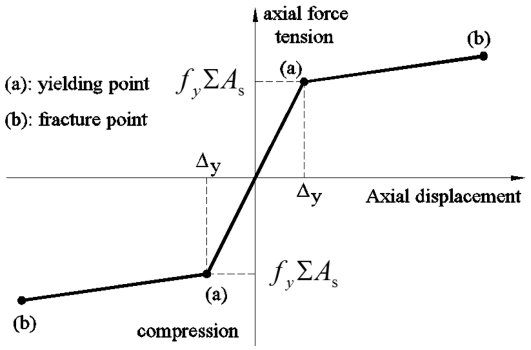

Fig. 7 Backbone curve for steel spring

2.3.2 Steel sub-spring

The steel sub-spring represents the behavior of steel reinforcement in the zone of plastic hinge. The yield force of the spring is $f_y\Sigma A_s$. The elastic and plastic stiffness of the spring are equal to $E_s(\Sigma A_s)/L_p$ and $E_p(\Sigma A_s)/L_p$, respectively. The backbone curve that governs the behavior of steel sub-spring is shown in Fig. 7.

2.3.3 Lap splice spring and anchorage bond slip spring

The tri-uniform bond stress model described in the companion paper was used to construct the steel stress-slip relation for the lap splice spring. Fig. 8 shows the backbone curve that governs lap splice spring behavior. The failure of lap splice can be classified as either "pre-yield" or "post-yield" splitting failure depending on the state of stress in the bar at failure. The failure is "pre-yield" if splitting failure occurs before steel yields, otherwise the failure is "post-yield". In the figure, c_0 is assumed to be the distance between ribs on deformed bar surface.

The anchorage bond slip spring plays essentially the same role as the lap splice spring, that is, it produces an extra deformation due to pull out slip of reinforcing bars embedded into footing. However, unlike the lap splice which fails by splitting mode, the failure of an anchored bar is presumed to be pull-out mode, i.e., line 1 in Fig. 9. Since the pull-out failure provides the largest bond strength, the bar will normally develop yield strength provided that it is sufficiently embedded

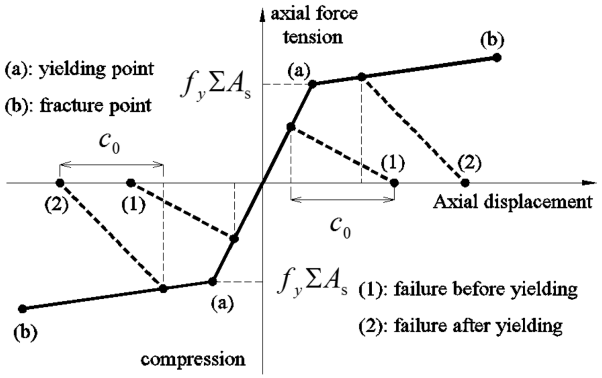

Fig. 8 Backbone curve for lap splice spring

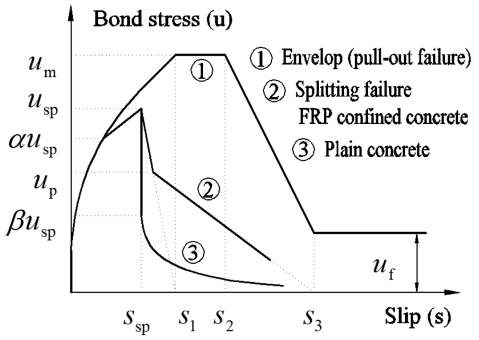

Fig. 9 Bond stress-slip model (Harajli 2006b)

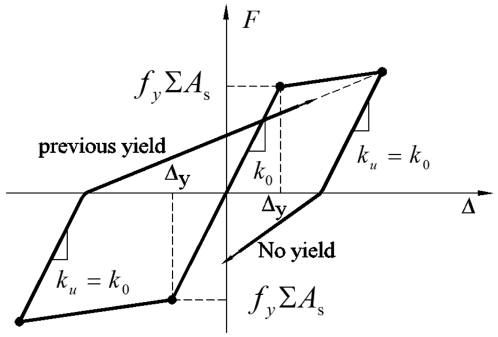

Fig. 10 Modified Takeda Degrading hysteretic model for reinforcement spring (Carr 2005)

into the footing. Generally, the steel stress-pull out slip relation for the anchorage spring can be constructed in the same way as that for lap splice sub-spring. The modeling concept as outlined in the companion paper can be adopted with the length of lap splice replaced by the embedment length and splitting bond stress-slip model confined by FRP (line 2 in Fig. 9) replaced by pull-out bond stress-slip model (line 1 in Fig. 9).

The Modified Takeda Degrading Stiffness hysteresis model (Fig. 10) (Carr 2005) is employed to simulate the cyclic response of steel sub-spring, lap splice spring, and anchorage bond slip spring. The unloading stiffness k_u is assumed to be the same as the initial elastic stiffness k_0. The reloading curve tends to approach the nominal yield point (line "No yield") if steel has not yielded in the previous loop and approach the unloading point (line "previous yield") if the steel has yielded in the previous loop.

3. Verification of nonlinear modeling and analysis

3.1 Response of columns subjected to cyclic load tested by Harajli and Dagher (2008)

Harajli *et al.* (2008) conducted an experimental investigation on the use of external fiber reinforced polymer (FRP) confinement for bond strengthening of spliced reinforcements in rectangular reinforced concrete columns and the consequent effect on the seismic responses. Nine 0.2 m wide × 0.4 m deep × 1.5 m high columns were divided into 3 series based on steel diameter used. The 14 mm diameter series consisted of specimens C14FP1, C14FP2 and C14E; 16 mm diameter series consisted of specimens C16FP1, C16FP2 and C16E; and 20mm diameter series consisted of specimens C20FP1, C20FP2 and C20E. For each specimen label, suffixes "FP1" and "FP2" meant the number of FRP sheets, and suffix "E" meant the column with no lap splice. Each specimen consisted of eight longitudinal reinforcing bars with lap splice length of $30d_b$ at the base. The ratio of concrete cover to bar diameter c/d_b was 1.4, 2.1 and 1.0 for series C14, C16 and C20 respectively. Transverse steels were 8 mm diameter bars spaced at 200 mm throughout the height of the strengthened columns, while in the unconfined "E" column, the stirrups were 8 mm diameter bars spaced at 50 mm within 500 mm from the base and spaced at 100 mm in the remaining height. Yield strength of bars f_y in series C14, C16 and C20 were 550 MPa, 528 MPa and 617 MPa

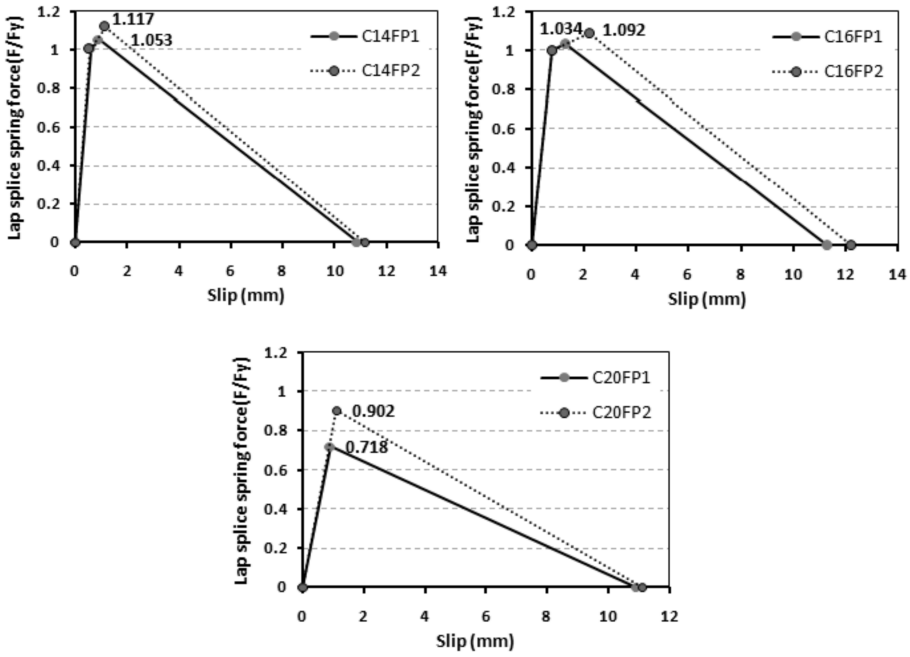

Fig. 11 Stress-slip relations for the lap splice spring

respectively. Compressive strength of concrete f_c' varied from 32 MPa to 40 MPa. The FRP sheets were 0.13 mm thick; with the elastic modulus of 230 GPa and the tensile fracture strain of 1.5%. The clear distance c_0 between the ribs on the bar surface was 10 mm.

Fig. 11 show the steel stress-slip relations for the lap splice spring derived from the tri-uniform bond stress model. As can be seen, in each series, the steel stress-slip relation is increased as the number of FRP layers increases. The model predicts the lap splice failure in the post-yield range for series 14 and 16 (the lap splice strength is larger than the yield strength), but predicts splitting failure in the pre-yield range for series 20. The analysis is also conducted for three specimens C14E, C16E and C20E which possess the same configuration as the wrapped columns except the longitudinal bars are continuously embedded into footing without lap splice. The lap splice springs are excluded from the analytical model to simulate these columns. The comparison between nonlinear analyses and experimental results are shown in Fig. 12 to Fig. 14. In these figures, the thick dotted black line denotes the envelope of the analysis cases in which the lap splice spring is excluded from the model but other effects of confinement including confined concrete strength are taken into account. In each of these figures, the grey curve denotes the experimental result, and the black line denotes the analysis result.

As can be seen, the predicted cyclic responses including lap splice springs are in general close to the experimental results for all columns. The analysis correctly captures the experimental trend, that is, the lateral strength and ductility of column increase with increasing number of FRP sheets. The ductility is increased because the bar is stressed to yielding without prior splitting failure. It is evident from these figures that without including the lap-splice spring, the analysis wrongly overestimates the load-deflection responses. Without properly accounting for the lap splice failure, the analysis predicts unconservatively high ductility and strength which may lead to the erroneous

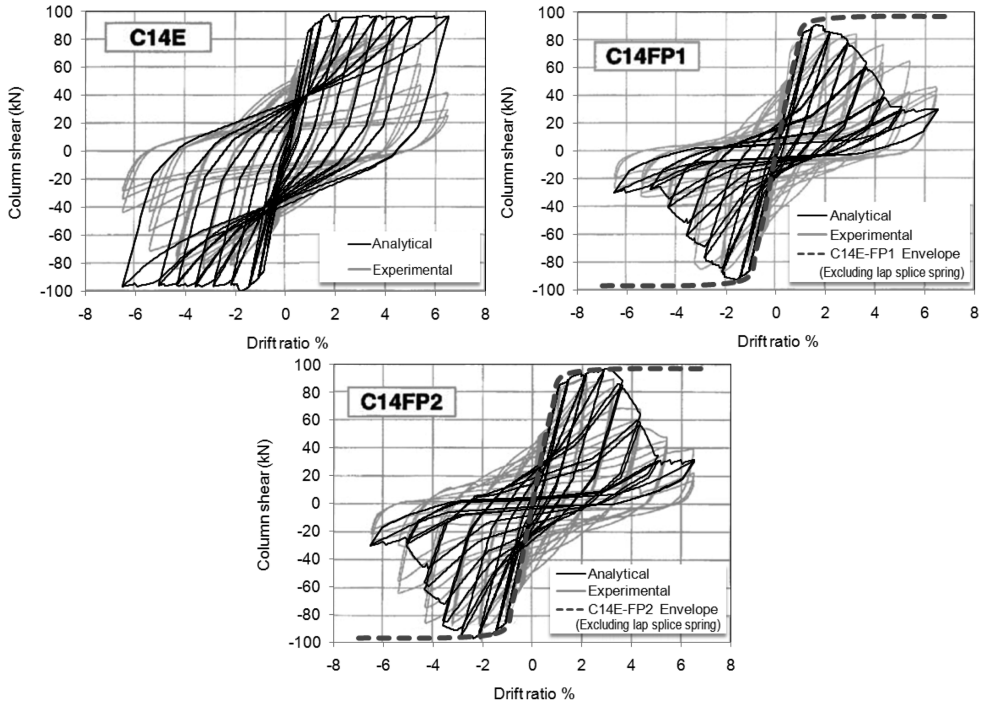

Fig. 12 Response of columns C14E, C14FP1and C14FP2

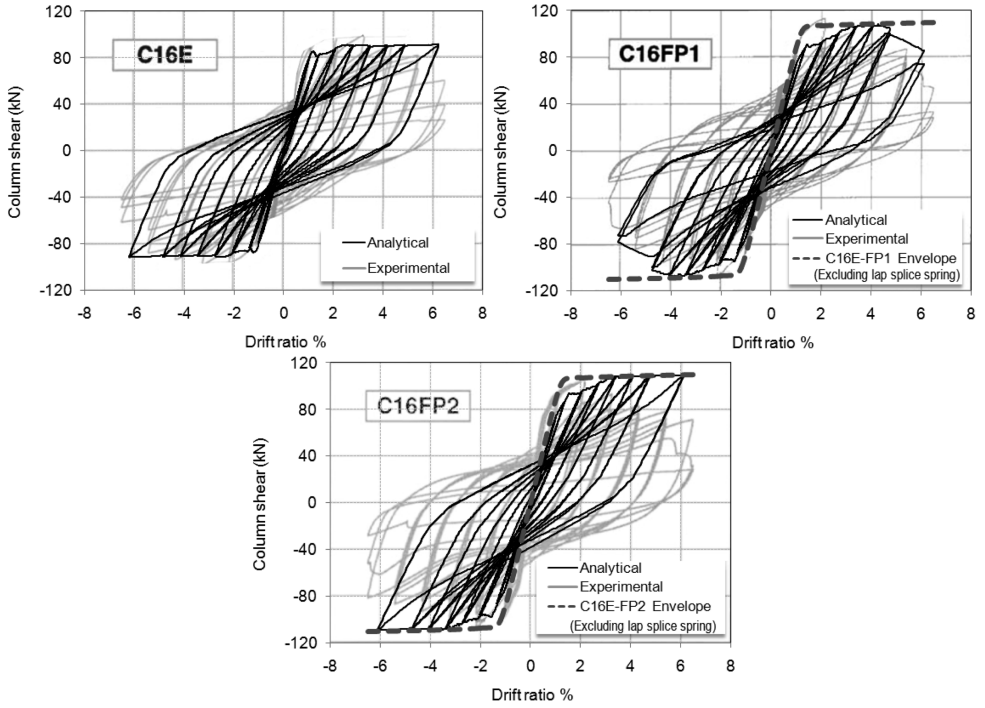

Fig. 13 Response of columns C16E, C16FP1 and C16FP2

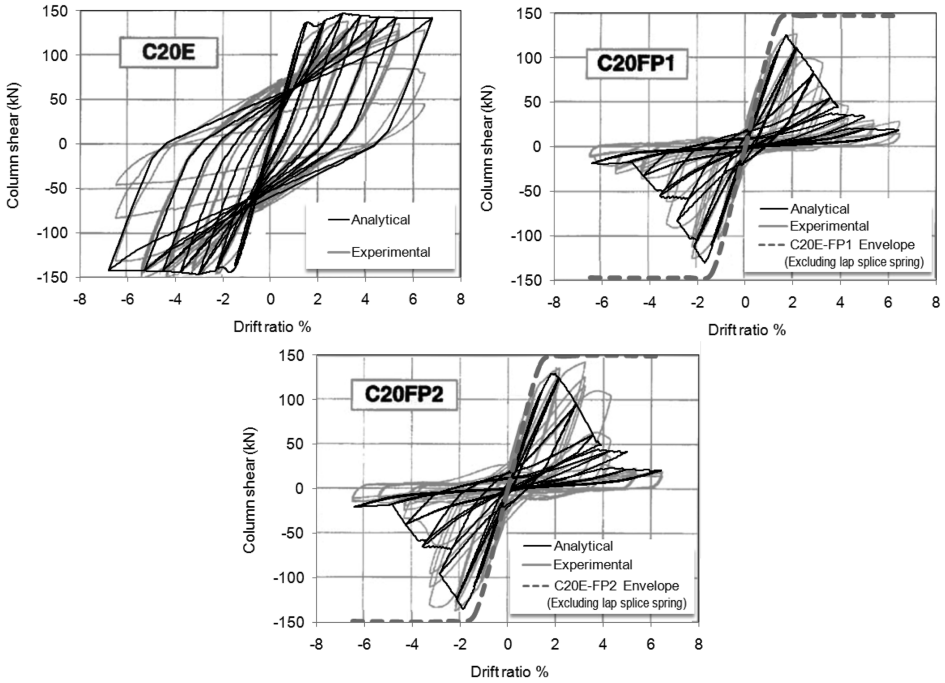

Fig. 14 Response of columns C20E, C20FP1 and C20FP2

Table 1 Verification with Harajli's experimental results (Harajli *et al.* 2008)

Specimen	Lateral force			Type of lap splice failure	
	Experiment	Analysis	Difference	Experiment	Analysis
C14FP1	87.2	92.3	1.06	After yielding of bar	After yielding of bar
C14FP2	92.2	97.2	1.05	After yielding of bar	After yielding of bar
C14E	84.3	100.0	1.19		
C16FP1	112.5	108.0	0.96	After yielding of bar	After yielding of bar
C16FP2	107.4	109.0	1.01	After yielding of bar	After yielding of bar
C16E	97.9	91.6	0.94		
C20FP1	126	130.0	1.03	Before yielding of bar	Before yielding of bar
C20FP2	141.8	135.0	0.95	Before yielding of bar	Before yielding of bar
C20E	150.7	147.0	0.98		
		Average	1.02		
		S.D	0.08		

interpretation in the performance assessment. Table 1 shows a comparison of column lateral strength between analysis results and experimental ones. The difference between analytical and experimental lateral strengths varies in an acceptable range of 10%. The comparison of failure modes between experiment and analysis is also provided. An excellent prediction of the failure mode can be seen.

3.2 Response of columns subjected to cyclic load tested by Xiao et al. (1997)

An experimental study on seismic retrofit of reinforced concrete circular columns with poor lap splice detail using prefabricated composite jacketing has been conducted by Xiao *et al.* (1997). The experiment consisted of three half-scale circular column specimens C1-A, C2-RT4 and C3-RT5. All specimens were 2.44 m high and had 0.61 m diameter. Specimen C1-A was a control specimen without any wrappings (as-built condition) and the other two columns C2-RT4 and C3-RT5 were tested after being strengthened with 4 and 5 prefabricated jacketing layers. Longitudinal reinforcements were 20 deformed No. 6 bars (d_b = 19.1 mm) grade 60 (f_y = 462 MPa) with 2%

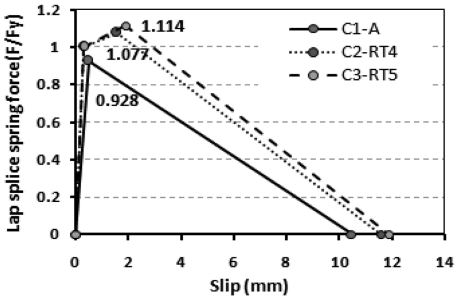

Fig. 15 Steel stress-slip relations of the lap splice spring

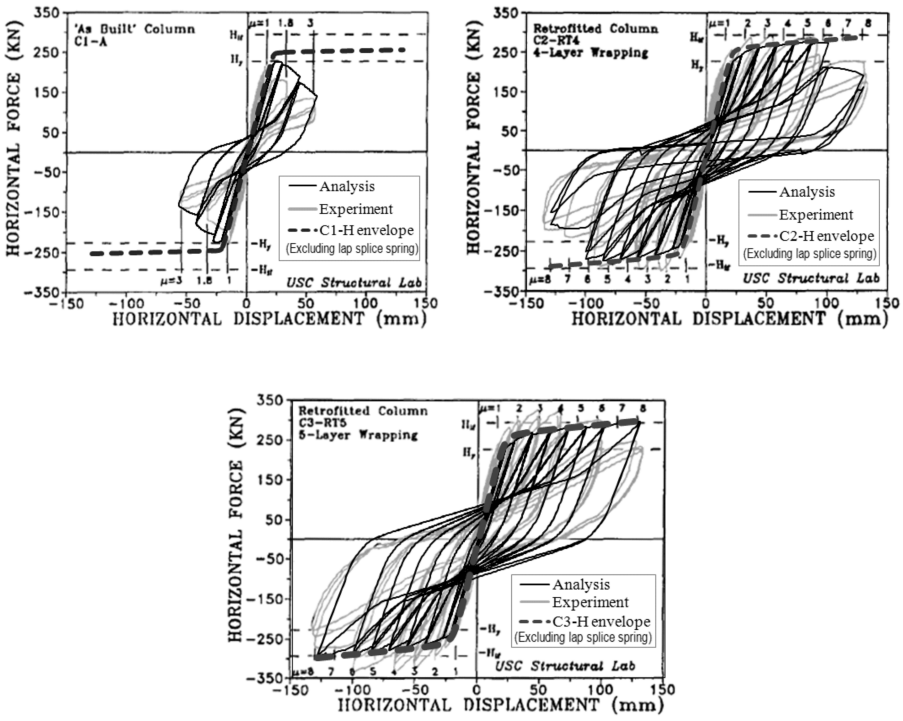

Fig. 16 Response of columns C1-A, C2-RT4 and C3-RT5

reinforcement ratio. The column bars were spliced with starter bars projected from the footing at the base with a lap length of 0.38 m ($20d_b$). The transverse reinforcements consisted of round No. 2 hoops (ϕ6.4 mm) spaced at 127 mm center to center. Concrete strength was 44.8 MPa (standard cylindrical specimen). Composite jacketing layer was 3.2 mm thick prefabricated unidirectional glass fiber sheets. The elastic modulus and ultimate strength in the circumferential direction were 48300 MPa and 552 MPa, respectively. The FRP prefabricated plates were attached to the column's full length via two part chemical epoxy. The axial load applied to the column was 712 kN with the resulting axial force ratio $P/A_g f_c' = 5\%$.

Fig. 15 shows the steel stress versus slip of lap splice sub-spring constructed from the tri-uniform bond stress model. As shown, the lap splice strength of the as-built column (C1-A) is smaller than the yield strength. When the columns are wrapped by FRP sheets, the model predicts the increase in strength beyond the yield load up to 7.7% and 11.1% for specimens C2-RT4 and C3-RT5, respectively. The predicted responses of columns C1-A, C2-RT4 and C3-RT5 are compared with the experimental results in Fig. 16. As can be seen, a good agreement is obtained in all specimens in terms of strength, ductility and hysteretic loops. For the unwrapped column (column C1-A), the experiment demonstrated a brittle lap splice failure before yielding of steel bars. On the other hand, the wrapped columns showed a remarkable improvement in the responses. These failure modes are well predicted by the proposed tri-uniform bond stress model. The analyses of the companion hypothetical specimens without lap-splice springs are also conducted. The section and reinforcement details of these hypothetical columns were the same as their tested companion columns except the reinforcing bars are assumed to be continuously embedded into the footing. The envelopes of the hysteretic responses are displayed as thick dotted black envelopes in Fig. 16. It is apparent that without including the lap splice spring in the model, the calculation can be grossly overestimated especially in the column C1-A that failed by splitting failure before yielding. For the wrapped specimens (C2-RT4 and C3-RT5), the stress of bar could be developed into post yield range, hence there is no significant difference in strength between the analyses with and without lap splice sub-spring included. However, for specimen C2-RT4, the incorporation of lap splice sub-spring leads to a more correct prediction of the displacement ductility. Table 2 shows a comparison between experimental and analytical results of Xiao's columns. The maximum experimental lateral force of columns C1-A, C2-RT4 and C3-RT5 was 231, 290 and 330 kN while the analysis gave the values of 228, 276 and 289 kN respectively. The differences between results are 1%, 5% and 10% respectively.

Table 2 Verification with Xiao's experimental results (Xiao *et al.* 1997)

Specimen	Lateral force		
	Exper.	Analysis	Differ.
C1-A	231	228.0	0.99
C2-RT4	290	276.0	0.95
C3-RT5	330	298.0	0.90
		Average	0.95
		S.D	0.04

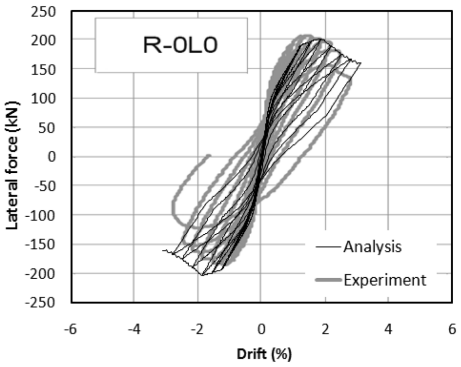

Fig. 17 Response of column R-0L0

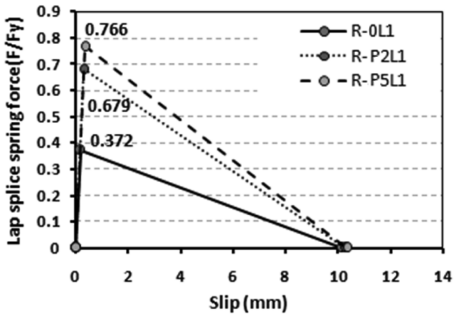

Fig. 18 Stress-slip relations for the lap splice in columns R-0L1, R-P2L1 and R-P5L1

3.3 Response of columns subjected to cyclic load tested by Bousias et al. (2006)

Six columns with lap splice zone confined by CFRP (carbon fiber reinforced polymer) sheets were tested by Bousias *et al.* (2006). The column section was 0.25 m wide and 0.50 m deep. The column longitudinal bars were 4-ϕ18-mm diameter steel bars with the yield strength f_y of 514 MPa. The location of the load application was 1.6 m above the base. The CFRP was 0.13 mm thick sheet and had 230 GPa elastic modulus and 3450 MPa tensile strength. Three columns R-0L1, R-P2L1 and R-P5L1 had the lap splice length of $15d_b$ and were tested under three conditions: as-built (no FRP), wrapped by 2 CFRP sheets and wrapped by 5 CFRP sheets respectively. The other three columns R-0L3, R-P2L3 and R-P5L3 had lap splice length of $30d_b$, and were tested under as built (no FRP), wrapped by 2 CFRP sheets and wrapped by 5 CFRP sheets respectively. The axial force applied on the top of columns varied from $0.23A_g f_c'$ to $0.3A_g f_c'$. The cylindrical compressive strength of concrete was 30 MPa.

Fig. 17 shows the comparison between the prediction and experimental hysteretic responses of column R-0L0 with neither lap splice nor FRP wrapping. The prediction seems to be good. Fig. 18 shows the backbone steel stress-slip relation of lap-splice springs that were used in the nonlinear analysis for $15d_b$ series. The model predicts the lap splice failure before yielding of steel bars in all columns even in specimen R-P5L1 that was wrapped by as many as 5 layers. With 2 layers of FRP, the strength enhancement is almost doubled compared with the unwrapped column. As the number of FRP sheets increases, the strength enhancement is however not proportionally increasing. Fig. 19 shows the cyclic responses of column R-0L1, R-P2L1 and R-P5L1 respectively. The corresponding envelopes for the column without lap-splice spring are shown as dotted black curves in the graph. In general, it can be seen that the analyses that include lap-splice sub-spring yield a good comparison with the experimental results. The experiment showed pre-yield splitting failures in all specimens as closely predicted by the model. Without lap splice spring, however, the analysis predicts yielding of column longitudinal bars with incorrectly much higher load capacity and ductility.

Fig. 20 shows the backbone steel stress-slip relations of lap splice springs that were used in the analysis of $30d_b$ series. The model predicts the pre-yield splitting failure for the unwrapped column (R-0L3). For the columns that are wrapped by 2 and 5 layers, the strength of lap splices is

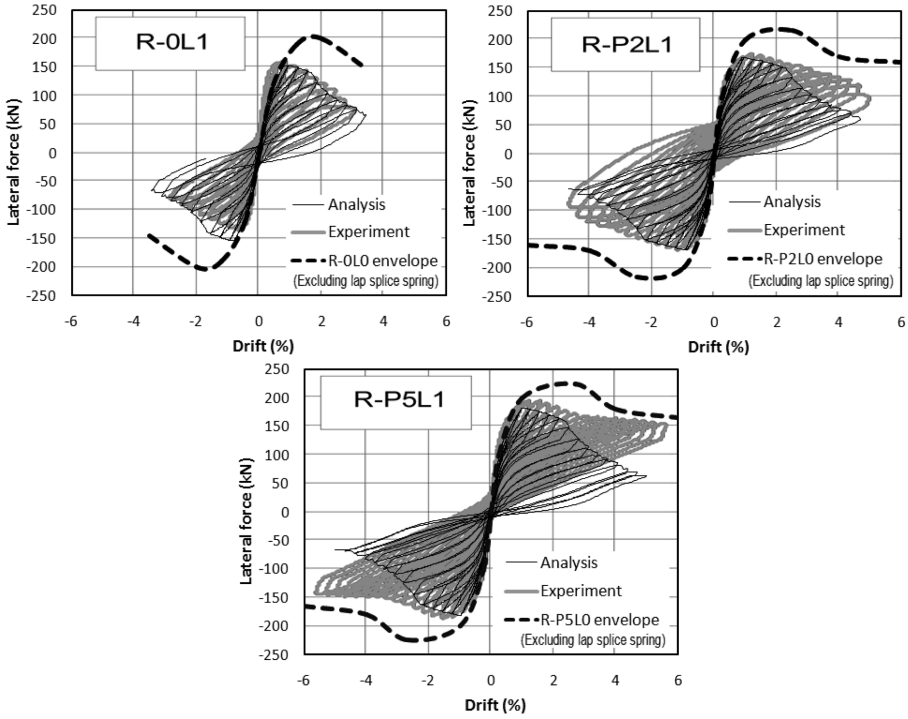

Fig. 19 Response of columns R-0L1, R-P2L1 and R-P5L1

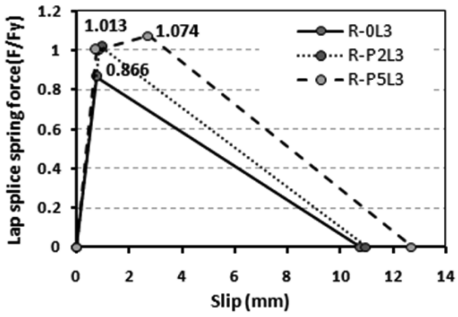

Fig. 20 Stress-slip relation for the lap splice in columns R-0L3, R-P2L3 and R-P5L3

developed into the post yield range. The cyclic responses of columns R-0L3, R-P2L3 and R-P5L3 are shown in Fig. 21. In these figures, the thick grey curves denote experimental results while the thin dark curves denote the analytical ones. A good agreement is obtained. The figure also shows the thick dotted black curves that represent the analytical envelopes of the corresponding wrapped columns, but without lap splice spring included in the analysis. As can be seen, for specimen R-0L3, the model predicts pre-yield splitting failure of lap splice, similar to the experiment. The analysis without lap splice spring yields a considerable overestimation in the lateral strength. For specimens R-P2L3 and R-P5L3, the FRP wrapping totally prevents the splitting failure and the peak lap splice strengths have not been reached (Fig. 20). In these cases, the specimens failed by

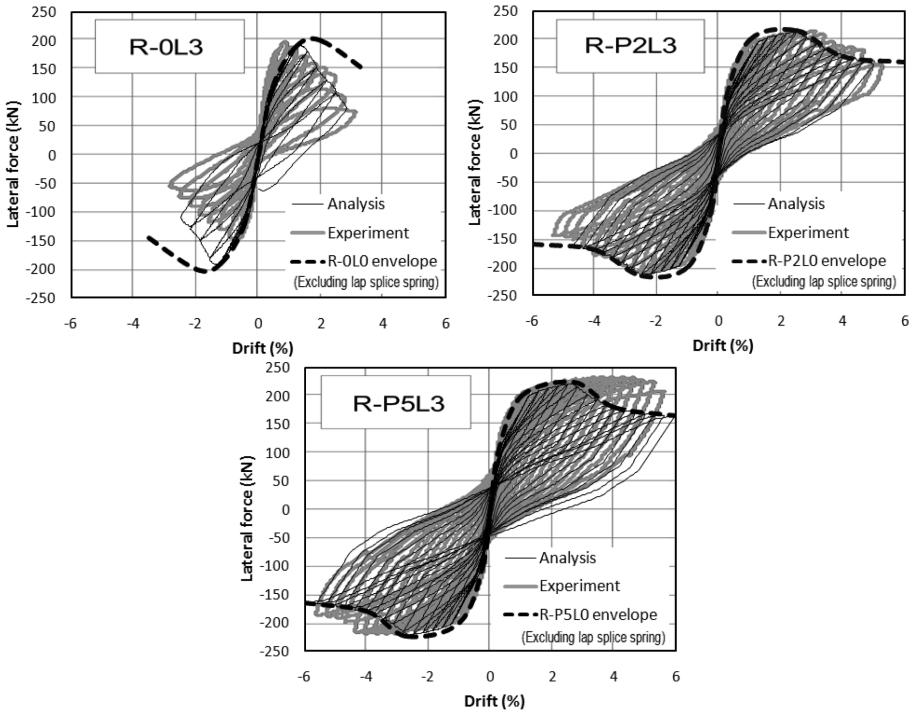

Fig. 21 Responses of columns R-0L3, R-P2L3 and R-P5L3

Table 3 Verification with Bousias's experimental results (Bousias *et al.* 2006)

Specimen	Lateral force (kN)		Difference
	Experiment	Analysis	
R-0L1	160	154.0	0.96
R-P2L1	175	168.0	0.96
R-P5L1	195	181.0	0.93
R-0L3	197.5	192.0	0.97
R-P2L3	215	214.0	1.00
R-P5L3	232.5	222.0	0.95
R-0L0	210	203	0.97
		Average	0.96
		S.D	0.02

concrete crushing due to a high axial force ratio (around 0.23-0.3 of axial capacity). Consequently, there is not much difference between the analyses with and without lap splice spring. Table 3 shows the comparison of column lateral strength between analytical and experimental results. The difference between them varies in a range of 7%.

4. Conclusions

The incorporation of steel stress-slip law is important for the nonlinear analysis of RC column with lap splice. A nonlinear modeling scheme is based on a discretization of column section into a number of fibers whose properties are represented by nonlinear concrete and/or steel springs. The steel springs are composed of three sub-springs, namely, steel bar sub-spring, lap splice sub-spring and anchorage bond slip sub-spring connected in series from top to bottom. These sub-springs are for modeling the response of steel bar, lap splice and anchorage of bars into footing respectively. The steel stress-slip relations for the confined lap splice have been constructed from the tri-uniform bond stress model. The anchorage bond slip sub-spring is constructed in the same way as the constitutive bond stress-slip model following the pull-out failure of reinforcing bars embedded into the footing. The verification of nonlinear modeling scheme and tri-uniform bond stress models has been performed through several cyclic load tests of columns conducted in previous studies. It is illustrated that the current modeling approach can correctly predict the hysteretic responses of columns subjected to cyclic displacement reversals. Without including the lap splice spring in the nonlinear analysis, the analysis may lead to an erroneous overestimation in the performance of the column especially for the ones with short lap splice length.

Acknowledgements

The authors are grateful to Thailand Research Fund for providing the research grant RSA 5280034. The second author would also like to express his appreciation to the Asian Development Bank (ADB), Japanese Government for granting the scholarship for his study at Sirindhorn International Institute of Technology, Thammasat University, Thailand.

References

ACI318 (2005), *ACI 318-05, Building Code Requirements for Structural Concrete and Commentary.*

ATC-40 (1996), *Seismic Evaluation and Retrofit of Concrete Buildings,* Vol. 1, Applied Technology Council.

Binici, B. and Mosalam, K.M. (2007), "Analysis of reinforced concrete columns retrofitted with fiber reinforced polymer lamina", *Compos. Part B-Eng.,* **38**(2), 265-276.

Bousias, S., Spathis, A.L. and Fardis, M.N. (2006), "Concrete or FRP jacketing of columns with lap splices for seismic rehabilitation", *J. Adv. Concrete Technol., Japan Concrete Inst.,* **4**(3), 431-444.

Carr, A.J. (1998), "Ruaumoko - Program for Inelastic Dynamic Analysis", Department of Civil Engineering, University of Canterbury, Christchurch, New Zealand.

Carr, A.J. (2005), "RUAUMOKO Manual", Department of Civil Engineering, The University of Canterbury, Christchurch, New Zealand.

Chai, Y., Priestley, M. and Seible, F. (1991), "Seismic retrofit of circular bridge columns for enhanced flexural performance", *ACI Struct. J.,* **88**(5), 572-584.

Cho, J.Y. and Pincheira, J.A. (2006), "Inelastic analysis of reinforced concrete columns with short lap splices subjected to reversed cyclic loads", *ACI Struct. J.,* **103**(2), 280-290.

Harajli, M.H. (2006a), "Axial stress-strain relationship for FRP confined circular and rectangular concrete columns", *Cement Concrete Compos.,* **28**(10), 938-948.

Harajli, M.H. (2006b), "Effect of confinement using steel, FRC, or FRP on the bond stress-slip response of steel bars under cyclic loading", *Mater. Struct.,* **39**, 621-634.

Harajli, M.H. (2008), "Seismic behavior of RC columns with bond-critical regions: criteria for bond strengthening using external FRP jackets", *J. Compos. Constr.,* **12**(1), 69-79.
Harajli, M.H. and Dagher, F. (2008), "Seismic strengthening of bond-critical regions in rectangular reinforced concrete columns using fiber-reinforced polymer wraps", *ACI Struct. J.,* **105**(1), 68-77.
Harajli, M.H., Hantouche, E. and Soudki, K. (2006), "Stress-strain model for fiber-reinforced polymer jacketed concrete columns", *ACI Struct. J.,* **103**(5), 672-682.
Kim, T.H., Kim, B.S., Chung, Y.S. and Shin, H.M. (2006), "Seismic performance assessment of reinforced concrete bridge piers with lap splices", *Eng. Struct.,* **28**(6), 935-945.
Matrin, S. (2007), "Nonlinear modeling of gravity load designed reinforced concrete buildings for seimic performance evaluation", Msc degree, Civil Engineering Department, Asian Institute of Technology, Bangkok, Thailand.
Melek, M., Wallace, J.W. and Conte, J.P. (2003), "Experimental assessment of columns with short lap-splice subjected to cyclic loads", PEER Report 2003/04, Pacific Earthquake Engineering Research Center, University of California, Berkeley.
Ogura, N., Bolander, J.E. and Ichinose, T. (2008), "Analysis of bond splitting failure of deformed bars within structural concrete", *Eng. Struct.,* **30**(2), 428-435.
Priestley, M.J.N. and Seible, F. (1991), "Seismic assessment and retrofit of bridges", *University of California, San Diego (SSRP),* **91**(03), 84-149.
Roy, H.E.H. and Sozen, M.A. (1965), "Ductility of concrete", *Am. Concrete Inst.,* **12**, 213-235.
Xiao, Y. and Ma, R. (1997), "Seismic retrofit of RC circular columns using prefabricated composite jacketing", *J. Struct. Eng.,* **123**(10), 1357-1364.

Notations

A_g : Gross area of section
A_c : Area of concrete in a fiber
A_{cc} : Area of concrete core
A_s (ΣA_s) : Area of reinforcement (total in fiber)
c : Concrete cover depth.
c_0 : Distance between the ribs of the reinforcing bar
d_b : Diameter of reinforcing bar
E_c : Modulus of elasticity of concrete
E_p : Plastic stiffness of reinforcement
E_s : Modulus of elasticity of reinforcement
f_s : Stress in longitudinal reinforcement
f_y : Yield stress of longitudinal reinforcement
F_c : Peak compressive strength of concrete spring
f_c' : Compressive strength of unconfined concrete
f_{cc}' : Compressive strength of confined concrete
f_{lf} : Lateral passive confining pressure exerted by FRP
f_{ls} : Lateral passive confining pressure exerted by transverse steel
g : Gap at the bottom of FRP jacket
H : Height of the column
I_g : Gross moment of inertia of the section
k_0 : Initial elastic stiffness of hysteretic model
k_1, k_2 : Confinement effectiveness coefficients
k_u : Stiffness of the unloading curve
L_p : Length of plastic hinge
P : Axial load applied on column
s_1, s_2, s_3 : Local slip parameters in the bond stress-slip model
s_{sp} : The slip at bond splitting failure
u_f : The residual bond strength
u_m : Maximum bond stress at pullout mode
u_p : Bond stress parameter in the bond stress-slip model
u_{sp} : Peak bond stress in the bond stress-slip model
ε_0 : Strain at maximum stress of unconfined concrete
ε_{50} : Strain at concrete stress of 50% of the peak concrete stress
ε_{co} : Concrete strain at the intersection point between the 1st and 2nd stage of the stress-strain curve
ε_{cc} : Concrete strain for confined concrete
ε_{cu} : Limiting concrete strain
Δy : Yield displacement